

Piatti, E., Sola, A., Daghero, D., Ummarino, G. A., Laviano, F., Nair, J. R.,  
Gerbaldi, C., Cristiano, R., Casaburi, A., and Gonnelli, R. S. (2016)  
Superconducting transition temperature modulation in NbN via EDL gating.  
Journal of Superconductivity and Novel Magnetism

There may be differences between this version and the published version. You are  
advised to consult the publisher's version if you wish to cite from it.

<http://eprints.gla.ac.uk/114667/>

Deposited on: 22 January 2016

# Superconducting transition temperature modulation in NbN via EDL gating

E. Piatti · A. Sola · D. Daghero · G. A. Ummarino · F. Laviano · J. R. Nair · C. Gerbaldi · R. Cristiano · A. Casaburi · R. S. Gonnelli

Received: date / Accepted: date

**Abstract** We perform electric double layer gating experiments on thin films of niobium nitride. Thanks to a cross-linked polymer electrolyte system of improved efficiency, we induce surface charge densities as high as  $\approx 2.8 \times 10^{15} \text{cm}^{-2}$  in the active channel of the devices. We report a reversible modulation of the superconducting transition temperature (either positive or negative depending on the sign of the gate voltage) whose magnitude and sign are incompatible with the confinement of the perturbed superconducting state to a thin surface layer, as would be expected within a naïve screening model.

**Keywords** EDL gating · Superconductivity · Thin films · Niobium nitride · Screening

In recent years, electric double layer (EDL) gating has become a popular tool in condensed matter physics to tune the chemical potential of a wide range of materials well beyond the capabilities of standard solid-gate field-effect devices. Indeed, the EDL that builds up at the interface between the active channel and a polymer electrolyte solution (or an ionic liquid) acts as an effective nanoscale capacitor with extremely high capacitance [1]. In the field of superconductivity, EDL

gating has been shown to rival the effects of standard chemical doping in its capabilities to modify the properties of various materials [2]. So far, the attention has been focused on relatively low-carrier-density systems, where the electric field effect is stronger. Superconductivity induced by EDL gating was first reported in undoped  $\text{SrTiO}_3$  [3], then in  $\text{ZrNCl}$  [1] and more recently in  $\text{MoS}_2$  [4]. A Mott-insulator-to-metal transition was induced in the iron chalcogenide  $\text{TlFe}_{1.6}\text{Se}_2$ , though the induced carrier density was not sufficient to induce superconductivity [5]. Robust control on the transition temperature of cuprates was also claimed [6–8].

On the contrary, investigation of the effects of EDL gating on strongly metallic compounds in general, and standard BCS superconductors in particular, has insofar been lacking, probably because the electric field is expected to be strongly screened in such materials. Even so, our earlier experiments on gold [9] and other noble metals [10] have shown that it is possible to obtain reversible resistance modulations as high as 10% at low temperature in these systems.

Electric field effect in BCS superconductors exploiting a standard gating technique with a solid dielectric [11] or a ferroelectric gating [12] was already investigated in the Sixties. Those seminal works showed a small but detectable modulation of the superconducting transition temperature, compatible with the increase / decrease of the density of charge carriers.

In this work, we present the results of field-effect experiments in 40-nm thick films of the standard strong-coupling electron-phonon superconductor niobium nitride (NbN). With respect to the early papers mentioned above, the use of the EDL technique with a specifically designed cross-linked polymer electrolyte system (PES) allows inducing much higher charge densities. Small, but clearly detectable shifts in the supercon-

---

E. Piatti · A. Sola · D. Daghero · G. A. Ummarino · F. Laviano · J. R. Nair · C. Gerbaldi · R. S. Gonnelli  
Department of Applied Science and Technology, Politecnico di Torino, Italy

R. Cristiano  
CNR-SPIN Institute of Superconductors, Innovative Materials and Devices, UOS-Napoli, Italy.

A. Casaburi  
School of Engineering, University of Glasgow, UK

G.A. Ummarino  
National Research Nuclear University MEPhI (Moscow Engineering Physics Institute)

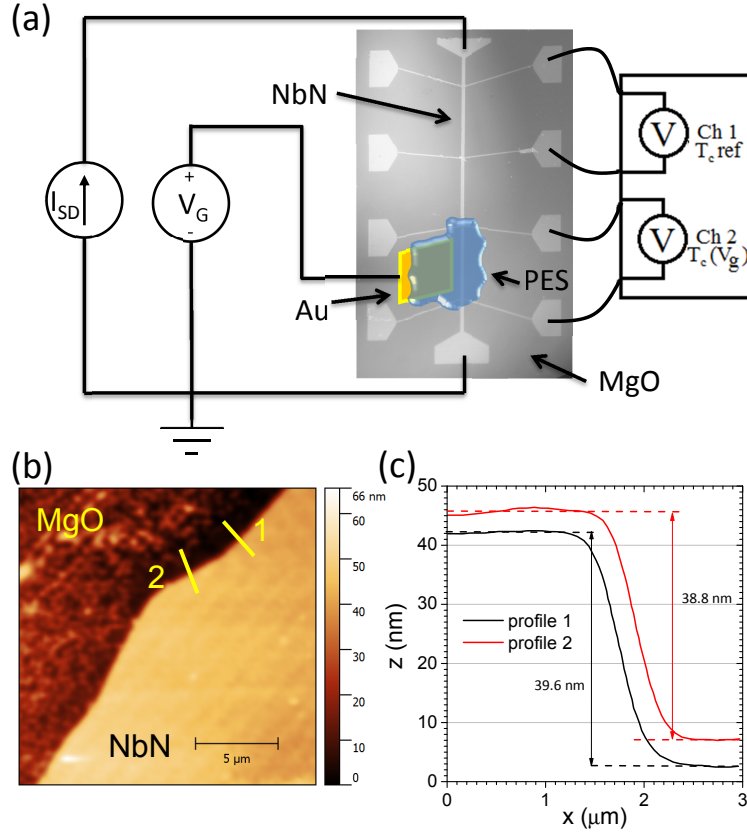


**Fig. 1** (a) Layout of the NbN field-effect device with a scheme of the electric connections for measurements of the gate current and of the resistance of the active and reference channels (ch. 2 and 1, respectively). (b) AFM image of the edge of one channel. (c) Height profile along the cuts in panel (b).

ducting transition temperature are induced upon electron depletion and accumulation in the active channel of our field-effect devices. The sign of these shifts is in agreement with an electrostatic modulation of the density of states of the material in the vicinity of its unperturbed value. However, a simple naïve model in which the perturbation is confined to the very surface of the film because of Thomas-Fermi screening is absolutely incompatible with the experimental findings, and more complex explanations are necessary to account for the results.

NbN thin films were grown on insulating MgO substrates by reactive magnetron sputtering and were patterned in a Hall-bar geometry by photolithography and wet etching in a 1:1 HF:HNO<sub>3</sub> solution. A patterned film is shown in figure 1a; the strip is 135  $\mu\text{m}$  wide and is divided into three identical, 946  $\mu\text{m}$  long “channels” in series (each delimited by adjacent voltage contacts). Surface quality and film thickness were characterized by atomic force microscopy (AFM) after device patterning. Figure 1b shows a  $17 \times 17 \mu\text{m}^2$  AFM scan of the edge

of the strip. An analysis of the film surface far from the edge shows an average roughness of about 1 nm. Figure 1c shows the  $z$ -profile of the film measured along the straight lines crossing the edge shown in panel (b). The film thickness, averaged over several similar cuts in different regions, turns out to be  $t = 39.2 \pm 0.8 \text{ nm}$ .

The shape of the sample allows us to measure at the same time the voltage drop (and thus the resistance) across two of the three channels when a dc current  $I_{SD}$  flows across the strip, as shown in the sketch of figure 1a. The resistance measurements were carried out in a two-stage pulse-tube cryocooler, from 300 K down to 2.7 K. The dc source-drain current  $I_{SD}$  was always between 10 and 50  $\mu\text{A}$ , which ensures a reliable measurement of  $T_c$  without appreciable shifts due to heating or critical current effects. Thermoelectric voltages were eliminated by inverting the current within each measurement [9]. Figure 2a shows the typical  $R(T)$  curve of any one channel, which exhibits the non-monotonic behavior characteristic of granular NbN films [13]. The critical temperatures determined at 10% and 90% of the

resistive transition are  $T_c^{10} = 14.91 \pm 0.02$  K and  $T_c^{10} = 14.99 \pm 0.02$  K, respectively. The uncertainties account for the reproducibility of the measurements in different thermal cycles. As discussed elsewhere [13] the residual resistivity ratio  $RRR = R(300\text{K})/R(16\text{K}) = 1.05$  indicates that the film quality is fairly high. In any case, the critical temperature of NbN has been proven to be primarily governed by carrier density rather than disorder scattering [14].

After this preliminary characterization of the film, we put the gate electrode (made of a rectangular leaf of gold) on the substrate, adjacent to one of the channels (the “active” channel). The liquid reactive mixture precursor of the PES was then drop-cast on top of the active channel and the neighboring gate, and UV-cured in a dry room. We chose the specific formulation of the PES from our earlier experiments on noble metals [9,10] owing to its record amount of charge induction: a mixture of bisphenol A ethoxylated dimethacrylate (BEMA) and poly(ethylene glycol) methyl ether methacrylate (PEGMA) in 3:7 ratio, with 10% wt of lithium bis-trifluoromethanesulfonimide (LiTFSI) and 3% wt of free radical photo initiator. The area of the Au gate electrode was always larger than that of the active channel, to ensure that the voltage drop across the EDL that forms on the active channel practically coincides with the whole applied gate voltage. In any case, the critical parameter in our experiments is the surface density of induced charges and not the gate voltage.

Field-effect measurements were initially made at room temperature, above the glassy transition of the PES (that occurs below 230 K), to determine the amount of charge induced by a given gate voltage  $V_G$ . A source-measure unit (SMU) was used to apply  $V_G$  and to measure the gate current; at the same time, we measured the resistance of the active and reference channels. When a positive (negative) gate voltage is applied, two things happen: i) the gate current shows a peak (dip) and then decreases (increases) finally saturating at an approximately constant value [9]. Even for the maximum gate voltages ( $\pm 3$  V), this current is  $10^4$  times smaller than  $I_{SD}$ ; ii) the active channel resistance shows a decrease (increase) that is perfectly reversible only as long as the gate voltage does not exceed  $\pm 3$  V (for which the relative resistance variation is 0.8%). Limiting the gate voltage to the range of reversibility ensures that only electrostatic effects are taking place, and allows avoiding unwanted electrochemical reactions at the active channel surface.

The induced charge density was determined by using the well-established electrochemical technique called double-step chronocoulometry (DSCC)[15] based on the fact that the gate current contains two contributions:

$I_{EDL}$  (which is due to the build-up of the electric double layer and decays exponentially in time) and  $I_{diff}$  (which is due to the diffusion of electroreactants and varies with the square root of time). Figure 2b shows the time dependence of the total charge that flows through the gate circuit  $Q_{tot} = Q_{EDL} + Q_{diff}$  (obtained by integrating the gate current from zero to  $t$ ) when a gate voltage is applied and then removed. In the inset,  $Q_{tot}$  is plotted (separately for the charge and discharge) as a function of  $t^{1/2}$ . The values of  $Q_{EDL}$  for charge and discharge (called  $Q_c$  and  $Q_d$  in figure 2b) are determined by the intercept of the asymptotic  $t^{1/2}$  trends of  $Q_{tot}$  (dashed lines) [15]. The surface density of charge carriers induced in the active channel is thus given by  $n_{2D} = (Q_c + Q_d)/2eS$ , where  $e$  is the elementary charge and  $S$  is the area of the gated channel [9,10].

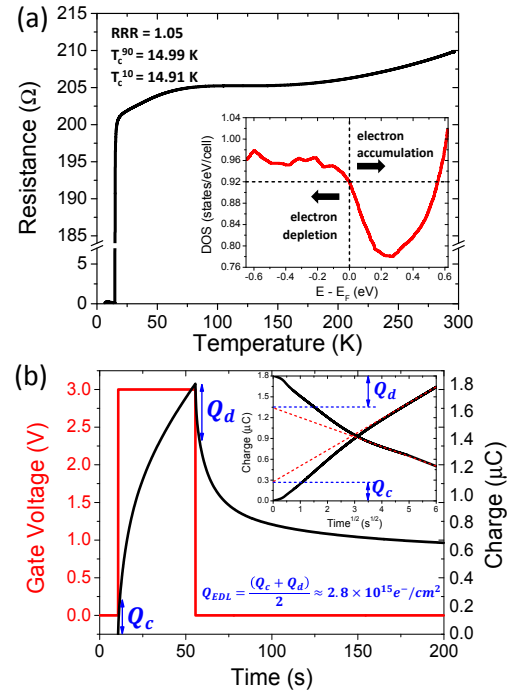


**Fig. 2** (a) Resistance of a channel (prior to PES drop-casting) as a function of temperature. Inset: computed DOS for NbN in the vicinity of the unperturbed chemical potential. (b) Charge flowing in the gate circuit,  $Q_{tot}$ , upon application and subsequent removal of  $V_G = +3.0$  V. Inset:  $Q_{tot}$  vs.  $t^{1/2}$  for charge and discharge. Dashed lines indicate the asymptotic  $t^{1/2}$  trends whose intercepts at  $t = 0$  determine  $Q_c$  and  $Q_d$ , which pertain to the charge and discharge of the EDL.

Once the value of  $n_{2D}$  corresponding to a given  $V_G$  was determined, we cooled down the device keeping  $V_G$  constant. Once the base temperature (2.7 K) was reached, the cryocooler was switched off and the  $R(T)$  curve of both the active and reference channels (ch. 2

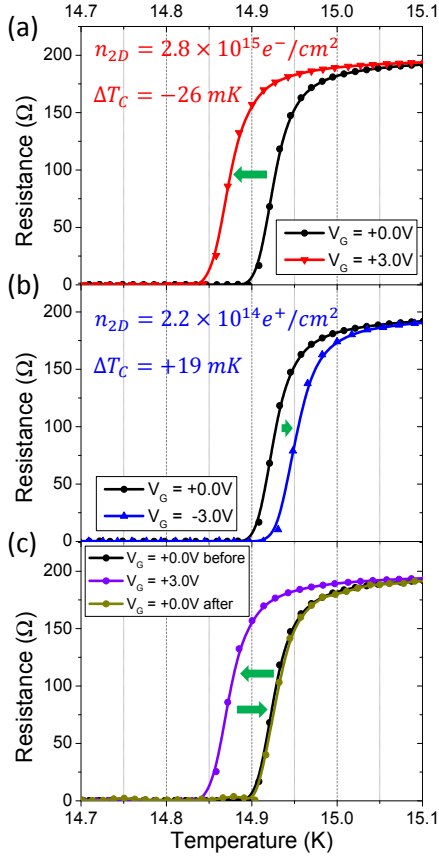


**Fig. 3** (a) Superconducting transition of the active channel for  $V_G = 0$  (black circles) and  $V_G = +3.0$  V (red triangles). (b) Same as in (a) but for  $V_G = 0$  (black circles) and  $V_G = -3.0$  V (blue triangles). (c) Reversibility check: superconducting transition of the active channel before (black), during (violet), and after (olive) application of  $V_G = +3.0$  V.

and 1 in figure 1a) was measured, in quasistatic conditions, during the very slow heating of the device up to room temperature. Using channel 1 as a reference allows detecting the shifts in the  $T_c$  of channel 2 with an improved sensitivity ( $\pm 2 \times 10^{-3}$  K) with respect to the absolute measure of  $T_c$  itself.

An extensive analysis of the  $T_c$  response to the charge induction is beyond the scope of this paper and will be discussed elsewhere. Here we only note that the amplitude of the  $T_c$  shift monotonically increases with  $n_{2D}$ , and we limit ourselves to the results obtained for  $V_G = \pm 3.0$  V, i.e. for the highest value of  $|V_G|$  that still ensures reversible effects. In these conditions the resistance of the active channel is modified by  $\pm 0.8\%$  with respect to that of the reference channel but there is no change in the *shape* of the  $R(T)$  curve – indeed, the shape is governed by the granular nature of the film and not by the density of charge carriers [13].

Let us now focus on the region of the superconducting transition. Figure 3a shows the  $R(T)$  curve of the active channel for  $V_G = 0$  (circles) compared to the same curve for  $V_G = +3.0$  V (down triangles) which corresponds to  $n_{2D} = 2.8 \times 10^{15}$  electrons/cm<sup>2</sup> according to DSCC. Note that the superconducting transition does *not* change shape or width, and is simply translated horizontally. In this particular case, the temperature shift is  $\Delta T_c = -26 \pm 2$  mK. Similarly, figure 3b shows the effect of a gate voltage  $V_G = -3.0$  V (corresponding to  $n_{2D} = 2.2 \times 10^{14}$  holes/cm<sup>2</sup>); in this case,  $T_c$  is enhanced by  $\Delta T_c = +19 \pm 2$  mK. A proof of the fact that these shifts are *only* due to electrostatic charge induction/depletion and not to chemical reactions, ions adsorption, surface degradation and so on, is provided in figure 3c that shows three subsequent  $R(T)$  curves measured with  $V_G = 0, +3.0$  V, 0 which clearly demonstrate the *complete reversibility* of the  $T_c$  shift.

The fact that electron accumulation gives rise to a *decrease* in  $T_c$  while electron depletion causes an *increase* in  $T_c$  can be qualitatively explained by looking at the density of states of NbN shown in the inset to figure 2a. The DOS was calculated with either the full-potential linearized augmented plane wave method or the pseudopotential method – as implemented in the Elk code [16] and in the Quantum Espresso package [17]. Around the unperturbed chemical potential  $\mu_0$  the DOS is asymmetric, i.e. it decreases when the chemical potential is increased (by means of electron accumulation) and vice versa. Within the Eliashberg theory of superconductivity, which is well obeyed by NbN (a standard strong-coupling electron-phonon superconductor with  $\lambda_{e-ph} = 1.437$  [14]), an increase (decrease) in the density of states at the Fermi level is expected to give rise to an increase (decrease) in  $T_c$ .

To calculate the shift of the chemical potential  $\mu - \mu_0$ , one needs to know the perturbation in the *volume* charge density,  $n_{3D}$ , but the experimentally accessible quantity is  $n_{2D}$  – which is the integral of  $n_{3D}(z)$  over the whole film thickness. The simplest, rough approximation for the  $n_{3D}(z)$  profile is a Heaviside step function:  $n_{3D}(z) = n_{3D}\Theta(\xi - z)$ ,  $\xi$  being the thickness of the perturbed layer. In NbN the Thomas-Fermi screening length is of the order of 1 Å, so that it is reasonable to take  $\xi \simeq 4.4$  Å, i.e. equal to the height of one unit cell. The resulting values of  $n_{3D}$  are reported in Table 1, as well as the corresponding shifts in the chemical potential  $\mu - \mu_0$ . We then solve the Eliashberg equations to calculate the expected  $T_c$  of the perturbed layer, assuming that the applied electric field does not affect the phonon spectrum, and modifies the electron-phonon spectral function and the Coulomb pseudopotential only through the DOS modulation.

**Table 1** Predictions of the simple parallel-channel model compared to experimental results. The assumed thickness of the perturbed layer is  $\xi = 4.4$  Å. The listed quantities are: the induced surface electron density (measured), the induced volume electron density, the chemical potential shift, the DOS ratio, the calculated and the measured  $T_c$  shift.

$n_{2D}$	$-2.2 \times 10^{14}$	$+2.8 \times 10^{15}$	$e^-/cm^2$
$n_{3D}$	$-4.4 \times 10^{21}$	$+6.8 \times 10^{22}$	$e^-/cm^3$
$\mu - \mu_0$	$-9.9 \times 10^{-2}$	$+1.14 \times 10^0$	eV
$N(\mu)/N(\mu_0)$	1.032	2.349	
$\Delta T_c, \text{calc}$	+0.650	+17.2	K
$\Delta T_c, \text{meas}$	$+1.9 \times 10^{-2}$	$-2.6 \times 10^{-2}$	K

Table 1 reports the values of the calculated  $T_c$  shifts for  $V_G = \pm 3$  V compared to the experimental ones shown in figure 3a,b. Although the calculated shifts refer only to the surface layer, nothing changes if the resistance of the whole film is calculated as the parallel of the perturbed and unperturbed layers. It is clear that the calculations completely fail to reproduce the experimental findings. For electron depletion ( $n_{2D} < 0$ ),  $\Delta T_c$  is overestimated by a factor  $\simeq 30$ . For electron accumulation ( $n_{2D} > 0$ ), the calculated chemical potential shift is so large that the system crosses the DOS minimum just above  $\mu_0$ , the DOS *increases* and  $T_c$  is hugely enhanced, in complete contrast with the experiment. Clearly, this means that the modulation of the superconducting properties is *not* limited to a surface layer of the order of one unit cell, as we have initially assumed.

Moreover, if the induced charge density was limited to a surface layer (no matter how thick), there would be *no way* to detect a suppression of the transition temperature (as we instead do in the case of electron accumulation, see table 1), since the underlying bulk would still become superconducting at a higher temperature, thus shunting the layer with locally depressed  $T_c$ . Such an observation can only be rationalized if the *whole* film thickness is somehow interested by the  $T_c$  shift. Understanding this effect requires a detailed investigation of the capability of the extremely high electric fields generated by EDL gating to penetrate inside a superconductor.

In conclusion, we performed EDL gating experiments on the standard strong-coupling electron-phonon superconductor NbN. Large densities of induced charge were obtained, up to  $+2.8 \times 10^{15}$  carriers/cm<sup>2</sup>, with a modulation of the room-temperature resistance up to several parts per thousand. We investigated the effect of the high electric field on the  $T_c$  of the material, and found it compatible in sign with small displacements of the chemical potential that would result in changes in the local DOS. However, the magnitude of the shift of  $T_c$  is

incompatible with a simple parallel-conducting-channel model in which the thickness of the perturbed layer is determined by the Thomas-Fermi screening length. Actually, the observation of a *negative* shift of  $T_c$  seems to indicate that the *whole* thickness of the film is perturbed. These findings pave the way toward a deeper understanding of the response of standard superconductors to strong electric fields. More generally, they might also help addressing the still pending problem of screening in materials subjected to the extreme conditions reachable in the EDL field effect devices.

## References

1. J. T. Ye et al., *Nature Mater.* **9**, 125-128 (2010)
2. K. Ueno et al., *J. Phys. Soc. Jpn.* **83**, 3, 032001 (2014).
3. K. Ueno et al., *Nature Mater.* **7**, 855-858 (2008)
4. J. T. Ye et al., *Science* **338**, 1193 (2012)
5. T. Katase et al., *Proc. Natl. Acad. Sci. U.S.A.*, **111**, 11 (2014)
6. A. T. Bollinger et al., *Nature* **472**, 458-460 (2011)
7. X. Leng et al., *Phys. Rev. Lett.* **107**, 027001 (2011)
8. X. Leng et al., *Phys. Rev. Lett.* **108**, 067004 (2012)
9. D. Daghero et al., *Phys. Rev. Lett.* **108**, 066807 (2012)
10. M. Tortello et al., *Appl. Surf. Sci.* **269**, 17 (2013)
11. R.E. Glover and M. D. Sherrill, *Phys. Rev. Lett.* **5**, 248 (1960)
12. H. L. Stadler, *Phys. Rev. Lett.* **14**, 979 (1965)
13. A. Nigro et al., *Phys. Rev. B* **37**, 3970 (1988)
14. Chockalingam et al., *Phys. Rev. B* **77**, 214503 (2008)
15. Inzelt, G. in *Electroanalytical Methods. Guide to Experiments and Applications 2nd edn.* (ed Scholz, F.), Ch. II.4 Chronocoulometry, 147-158 (Springer-Verlag, 2010)
16. <http://elk.sourceforge.net/>
17. P. Giannozzi et al. *J. Phys. Condens. Matter* **21**, 395502 (2009).